

SPIRE

SUBJECT: SPIRE Beam Steering Mirror Design Description

PREPARED BY: Ian Pain

DOCUMENT No: SPIRE-ATC-PRJ-000587

ISSUE: 3.4 **Date:** 07th February 2001

NOT APPROVED

APPROVED BY:

Date:

Local Project Manager: Ian Pain

Project Manager: Ken King

Instrument Scientist: Bruce Swinyard

Systems Engineer: John Delderfield

Colin Cunningham

Local Co-Investigator: Gillian Wright

REFERENCE: SPIRE-ATC-PRJ-002

SPIRE BEAM STEERING MIRROR DESIGN DESCRIPTION

v 3.4

Distribution List :

SPIRE-Project	Ken J. King	
	Bruce M. Swinyard	
	Matt Griffin	
UK ATC	Colin Cunningham	
	Gillian Wright	
	Ian Pain	
	David Henry	
	Brian Stobie	
	Richard Bennett	
	Tom Paul	
LAM	Didier Ferrand	
	Dominique Poulighen	
	Patrick Levacher	



FIRST

SPIRE

SPIRE Beam Steering Mirror Design Description
v 3.4

Ref: SPIRE-ATC-PRJ-002

Page : Page 2 of 38

Date : 7.Feb.01

Author: Ian Pain

Update

Date	Index	Remarks
5 Jun 2000	1	Creation of the document
28 Aug 2000	2	Revision of the document, internal to ATC
	3.1, 3.2.	Revision of the document, internal to ATC
12 Oct 2000	3.3	Revision – adding significant mechanical, electronics & controls content. Produced summary description for verbatim release in SPIRE-ATC-PRJ-001 and -003
02 Feb 01	3.4	Updated update table to include unreleased versions. Amended images to latest mechanical design state. Included flex pivot call out. Note electronics section requires substantial update to reflect progress.

Host system	Windows NT
Word Processor	Microsoft Word 97 sr-1
File	BSM Design Description v3_4.doc

1. Table of contents

<i>Distribution List</i> :	_____	1
<i>Update</i>	_____	2
1. <i>Table of contents</i>	_____	3
2. <i>Table of Figures</i>	_____	4
3. <i>Scope of the document</i>	_____	4
4. <i>Document List</i>	_____	5
4.1 Applicable documents	_____	5
4.2 Reference documents	_____	5
4.3 Glossary	_____	5
5. <i>Outline Description of the Beam Steering mirror mechanism subsystem</i>	_____	6
6. <i>Detailed Design Description of the Beam Steering mirror mechanism subsystem</i>	_____	8
6.1 The Cryogenic Mechanism (BSMm)	_____	8
6.1.1 Flex Pivots	_____	9
6.1.2 Finite Element Analysis (FEA)	_____	9
6.1.3 Flex Pivot Protection	_____	12
6.1.4 Dynamics	_____	13
6.2 The Support Structure (BSMs)	_____	14
6.2.1 Fasteners	_____	17
6.2.2 Materials	_____	17
6.2.3 Thermal Strap Connection	_____	18
6.2.4 Baffle and Light tight enclosure	_____	18
7. <i>BSM Electronics & Controls</i>	_____	19
7.1 Control System Design	_____	19
7.1.1 Parameters	_____	19
7.1.2 Dynamic Analysis	_____	19
7.1.3 Frequency analysis	_____	19
7.1.4 Damping	_____	20
7.1.5 Chop axis excitation	_____	20
7.1.6 Jiggle axis excitation	_____	21
7.1.7 Simulink Model	_____	23
7.1.8 Predicted Performance	_____	23
7.1.9 Power dissipation	_____	25
7.1.10 Rise time	_____	25
7.1.11 Positional Stability	_____	25
7.1.12 Gain and Phase Margins	_____	25
7.2 BSMe Electronics	_____	26
Block Diagram	_____	26
7.2.2 BSM Board	_____	27
7.2.3 Position sensors	_____	29
7.2.4 Position sensor read-out circuits	_____	29
7.2.5 Motors	_____	30
7.2.6 Thermometry	_____	31
7.2.7 Power Supply	_____	31
7.2.8 Grounding Scheme	_____	31
7.2.9 Harness/ Cables	_____	32
7.2.10 Interface to Digital Controller	_____	32

8. Reliability & Redundancy	33
8.1 Reliability Block Diagram	33
9. Command modes	35
9.1 Command List	35
Appendix i.	36
Appendix ii	37
Appendix iii Dynamic Analysis Of The BSM	38

2. Table of Figures

Figure 1 Photometer Layout, BSM in green, highlighted with yellow oval	6
Figure 2: View on underside of mirror - Chop stage grey, jiggle stage green, motors and sensors blue	8
Figure 3 FEA mesh for initial stiffness modelling	10
Figure 4: Flex pivot stresses from FEA	11
Figure 5 : Flex pivot protection sleeves, á la Goddard	12
Figure 6: Additional sketch of BSMs showing proposed mounting 'shoe' concept. Error! Bookmark not defined.	
Figure 8 BSMm and BSMs. 3D view from Pro/E model looking onto the mirror surface. Jiggle frame in green, coils in orange, sensors dark blue.	16
Figure 9: BSMm and BSMs. 3D view from Pro/E model looking from the rear. The PCAL unit is shown mounted at to the flat surface to the rear of the jiggle frame and motors.	16
Figure 10: Additional 3D view of BSM, showing mounting surface on underside. This interfaces to the proposed mounting 'shoe'	17
Figure 11: BSM shown with a conical baffle concept (shown semi transparent for clarity)	18
Figure 12 BSM jiggle axis simplified dynamics with digital controller	19
Figure 13: Chop axis excitation	20
Figure 14: Chop axis excitation	21
Figure 15: Jiggle axis excitation	22
Figure 16: Jiggle axis excitation	22
Figure 17: BSM chop axis simplified dynamics with no position feedback and estimated velocity damping.	23
Figure 18: Jiggle axis step response.	24
Figure 19: Jiggle axis step response.	24
Figure 20: step response with no feedback	25
Figure 21 Gain and Phase Margins for a) Chop axis and b) Jiggle axis	25
Figure 22: the basic architecture of the BSM Chop Axis, this is duplicated for the jiggle axis	26
Figure 23 Incorporation of the BSM electronics within the	27
Figure 24: Launch Latch/Damper Scheme	28
Figure 25 Current source (as used in ISOPHOT.)	29
Figure 26 Position sensor bridge	29
Figure 27 Instrumentation Amplifier.	30
Figure 28 Motor Power Amplifier (as for SMEC)	30
Figure 29 Reliability Block Diagram	33
Figure 30 Alternative Redundancy Scheme	36

3. Scope of the document

This document describes the design FIRST/SPIRE Beam Steering Mirror mechanism subsystem. The intent of the document is to incorporate all design information available at a given release date, and it is expected that the document will evolve significantly, on approximately a monthly basis, until the design is frozen.

Section 5 of this document provides a summary design description that is referenced complete into AD1 and RD5.

4. Document List

4.1 Applicable documents

	Title	Author	Reference	Date
AD1	SPIRE Beam Steering Mirror Mechanism Subsystem Specification v.1.0	D.Henry	SPIRE-ATC-PRJ-001	May 2000
AD2	SPIRE Development plan	K.King	???	

4.2 Reference documents

	Title	Author	Reference	Date
RD1	Instrument Requirements Document	B.M.Swinyard	SPIRE-RAL-PRJ-000034 Iss .30	May 2000
RD2	Instrument Development Plan	K.King	SPIRE WE Review viewgraphs	6 Dec 1999
RD3	Proposal for Beam Steering Mirror	R.Sidey	ATC contract no. 017693	
RD4	System Level Criticality	B.M.Swinyard	???	???
RD5	BSM Development Plan	Colin Cunningham/ Ian Pain	SPIRE-ATC-PRJ-003	1 June 2000

4.3 Glossary

AD	Applicable Document	MAC	Multi-Axis Controller
CEA	Commissariat à l' Energie Atomique	MCE	Mechanism Control Electronics
CDR	Critical Design Review	MGSE	Mechanical Ground Support Equipment
CNES	Centre National des Etudes Spatiales	MPIA	Max Planck Institute for Astronomy
CoG	Centre of Gravity	MSSL	Mullard Space Science Laboratory
CQM	Cryogenic Qualification Model	NA	Not Applicable
DDR	Detailed Design Review	OGSE	Optical Ground Support Equipment
DESPA	Département des Etudes SPAtiales	PFM	ProtoFlight Model
DM	Development Model	RAL	Rutherford Appleton Laboratory
DRCU	Digital Read-out and Control Unit	RD	Reference Document
EGSE	Electrical Ground Support Equipment	BSM	Beam Steering Mirror
FIRST	Far Infra Red Space Telescope	UK ATC	United Kingdom Astronomy Technology Centre
FPU	Focal Plane Unit	BSM	Beam Steering Mirror
FS	Flight Spare model	SPIRE	Spectral and Photometric Imaging REceiver
LAM	Laboratoire d'Astrophysique de Marseille	TBC	To Be Confirmed
FTS	Fourier Transform Spectrometer	TBD	To Be Defined
		WE	Warm Electronics

5. Outline Description of the Beam Steering mirror mechanism subsystem

The Beam Steering Mirror mechanism subsystem (BSM) is a critical part of the SPIRE Instrument. It is used to steer the beam of the telescope on the photometer and spectrometer arrays in 2 orthogonal directions, for purposes of fully sampling the image, fine-pointing and signal modulation.

The BSM comprises 4 main deliverables :

1. **The cryogenic mechanism** (BSMm).
2. **The structural interface** (BSMs).
3. **The warm electronics** (BSMe)
4. **Mass and optical alignment dummies** as required for SPIRE system level integration, (BSMd)

The position of the BSMm & BSMs are indicated in Figure 1.

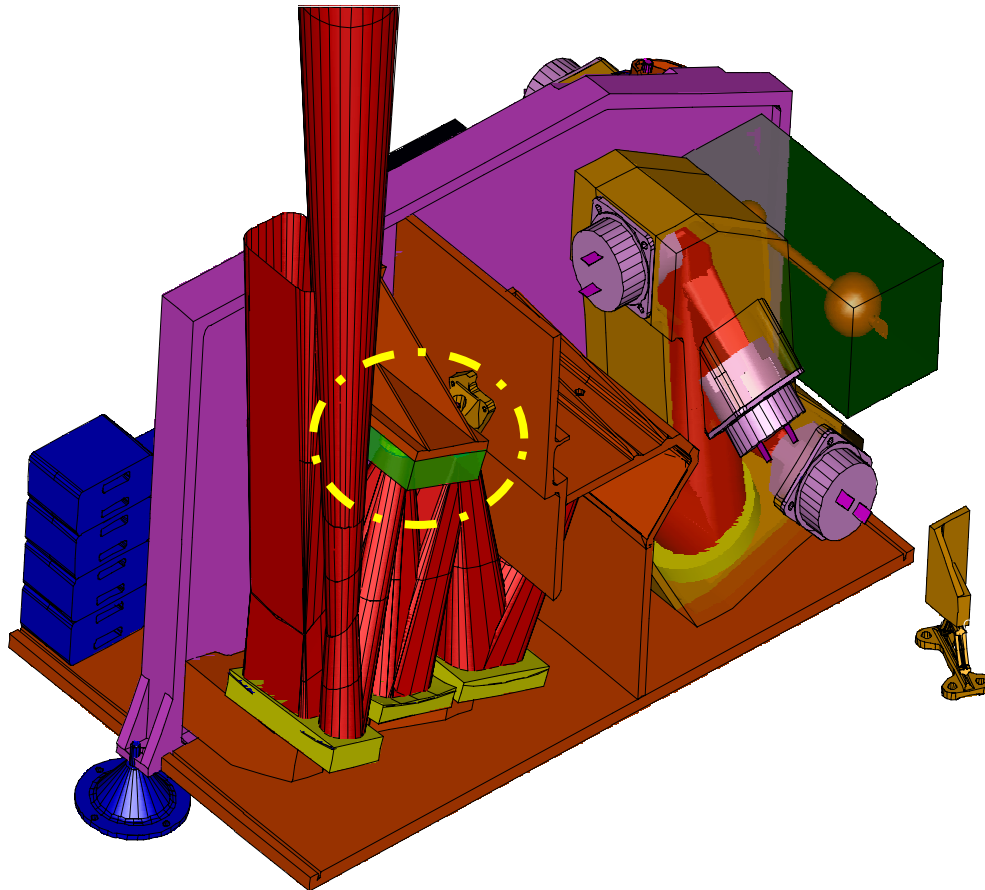


Figure 5-1 Photometer Layout, BSM in green, highlighted with yellow oval

The BSMs consists of an aluminium alloy mirror, nominal diameter 30mm, machined as part of the chop axis. This is mounted orthogonally within a gimbal-type frame which provides for jiggle axis motion. The axes are suspended by flex-pivot mounts.

The BSMs is a cryogenic device with nominal temperature 4K. Nominally, the chop axis provides 2.5 ° of mirror motion at 2 Hz and the jiggle axis provides 0.5° of motion at 1 Hz.

The BSM also provides an aperture through which the Photometer Calibration Source is directed towards the detector arrays.

The BSMs provides location of the BSMm on the SPIRE optical bench, and will also provide for a light tight enclosure and structural support for harnessing and thermometry. The BSMm integrates to the SPIRE Photometer Calibration Source (QMW), a baffle (RAL...TBC) and the SPIRE optical bench (MSSL). The BSMs is a cryogenic structure with nominal temperature 4K.

The BSMe provides electrical actuators are used to provide motion of the mirror. Electrical transducers are used to measure the mirror position to allow control of the mirror position. The BSMe baseline design makes use of cryogenic motors and magneto-resistive sensors used in ISOPHOT. Each axis houses a rare-earth (eg Cobalt-Samarium) magnet moving pole piece and is driven by a motor coil fixed to the mechanism housing/structure

The cryogenic electronics are connected to the analogue power and amplifier electronics on the Warm Electronics (WE) by a cryogenic harness which will also feed out signal cables from thermocouples on the BSMs. The BSM operates under control of the Detector Readout and Control (FSDRC) sub-system (LAM). The BSMe will be specified and designed by the UK ATC, then manufactured by LAM in conjunction with the SMEC electronics. Integration and test will be at LAM, with support from ATC.

The BSMd may comprise several actual dummies, with at least (1) an optical dummy for initial alignment work and (2) a mass-representative model for structural vibration tests. Designs for mass and optical alignment dummies will not be specified in detail until the BSMs/BSMm design is largely complete.

6. Detailed Design Description of the Beam Steering mirror mechanism subsystem

6.1 The Cryogenic Mechanism (BSMm)

The BSMm comprises a mirror of nominal diameter 30mm, mounted so as to pivot on two axes to provide chop and jiggle motion. Each axis houses a rare-earth (e.g. Cobalt-Samarium) magnet moving pole piece and is driven by a motor coil fixed to the mechanism housing/structure. Lucas flex-pivots, or equivalent, provide low friction motion and a small restoring torque.

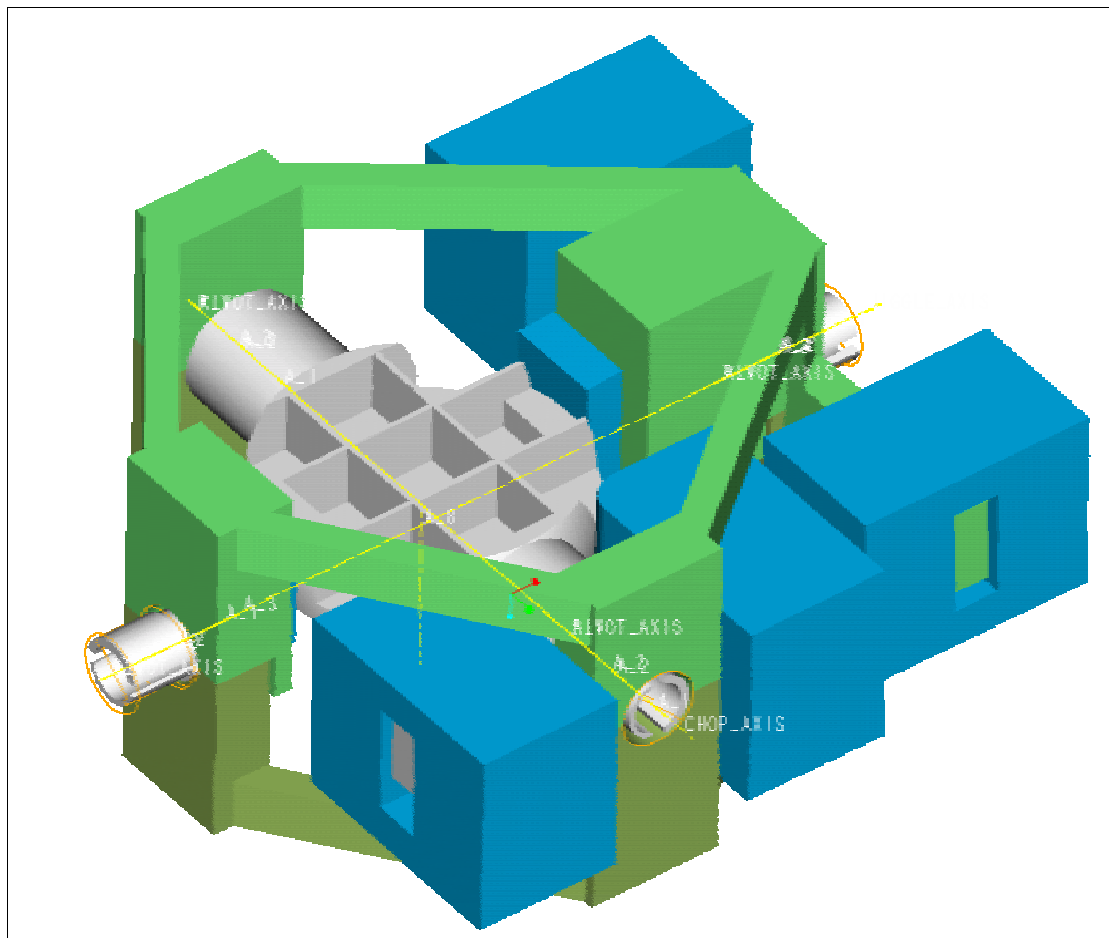


Figure 6-1: View on underside of mirror - Chop stage grey, jiggle stage green, motors and sensors blue

The chop and jiggle stages are shown in Figure 1. The chop stage is monolithic with the mirror machined integrally. The underside of the mirror is light-weighted and has pockets for the iron plates for the magneto-resistive position sensors. The chop direction is along the long axis of the array (the spacecraft y-axis). A **2mm diameter (TBC) hole** in the centre provides an optical path for the calibrator mounted behind the BSMm

The moment of inertia of the chop stage has been minimised to reduce power consumption during chop transitions. At 2.1 Kg.mm^2 , it is little more than the ISOPHOT rotor which was 1.57 Kg.mm^2 , resulting in an estimated power consumption of 0.4 mW when chopping at 2Hz with maximum amplitude. Mass is also minimised to keep loads on the flex pivots down during qualification and launch. Current estimate of static loads on the chop axis pivots with a 50g force is 9N, compared with pivot load capacity of 25N.

The jiggle stage is in the form of a split frame split and clamps together around the flex pivots. To balance the jiggle stage the framework in the opposite corner to the coils has been made solid. This also increases the stiffness of the structure. This structure carries the chop stage, and is inevitably heavier. Fortunately, the requirements call for lower amplitude and frequency in this axis, so we can use stiffer flexures, resulting in average power consumption of 1.6 mW when jiggling at 1 Hz with maximum amplitude. The static load on the jiggle axis flex-pivots at 50g is 27N, well below the 245N load capacity. The Pro/E solid model (shown) does not have light-weighting features modelled in the jiggle frame, though these may be seen in the FEA model shown later.

Both stages are designed to be stiff, so that the first resonant frequencies are high enough (> 700 Hz) that the system modelling can regard them as rigid bodies.

Space envelopes for the coils and sensors are shown in blue. There will be a 'primary' and 'cold redundant' motor for each axis. Depending on implementation, the motor for a single axis will either have:

- the prime coil on one side of the rocker beam and the redundant on the other, leading to an unbalanced load but a more rugged coil, or
- a balanced set of coils with the prime and redundant motor coils wound onto the same bobbin.

The coils may be potted (encapsulated) if required, and will certainly require extensive magnetic shielding and strong thermal linking to the thermal straps.

All the motor coils mount directly to the BSMs, i.e. the chop stage air gaps must be slightly over-size to accommodate chopping whilst in various jiggle modes. These inefficiencies have not yet been modelled.

Position sensors for the chop axis are mounted on the jiggle stage, which means flexible cable connections are required, unlike the jiggle stage position sensors, which mount directly on the non-moving housing. An alternative to this may be to place the chop axis sensor also to the housing and compensate for the movement in the jiggle axis in the look up table using this in conjunction with the jiggle axis position.

6.1.1 Flex Pivots

Two flex pivot types are envisaged, nominally supplied by Lucas Aerospace . The jiggle axis uses type 5010-800 and the chop axis the lighter 5010-600 units. As a minimum these would be cryogenic grade stainless steel, electron beam welded. Copper-berillium and inconel material choices are also possible and require further investigation. Final flex pivot specification is **TBD**.

6.1.2 Finite Element Analysis (FEA)

Initial FEA work of the structure and mirror has been performed to calculate approximate strength and resonant frequencies. The full report is found in ATC document, spire-bsm-001-tdn-001.doc see Appendix iii

6.1.2.1 Modelling

- The jiggle stage structure has been represented by thin shell elements;
- The chop stage has been represented by a tube of solid elements together with lumped masses (shown red in the illustration below) to give the same mass and moments of inertia as the solid model;
- The flex pivots have been modelled using a combination of solid and shell elements.

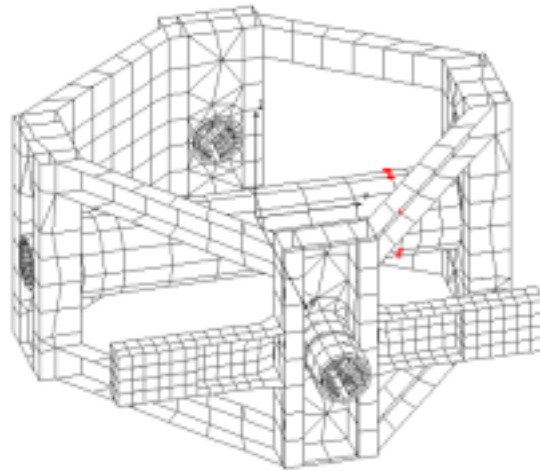


Figure 6-2 FEA mesh for initial stiffness modelling

- The jiggle stage framework between the flex-pivot housings has been modelled as 5mm x 5mm x 0.5mm channel section.
- The pivots have been moved as far as reasonably practical towards the mirror to minimise the inertia and maximise the stiffness. To clear the coils this leads to an asymmetric arrangement.
- To balance the jiggle stage the framework in the opposite corner to the coils has been made solid. This also increases the stiffness of the structure. Due to the use of lumped masses which do not give the correct products of inertia and also because the jiggle stage has not been dynamically balanced there will be some inaccuracy in modelling coupling of the stages.

6.1.2.2 Load cases

The following analyses have been made:

- 50 g static load in X,Y and Z directions
- Frequency response analysis for excitation of the chop and jiggle stages by couples of 1 Newton forces at the centre of the drive magnets (equivalent forces for the chop stage.)

6.1.2.3 Static stress analysis results

The three load cases (50g in X, Y and Z) lead to stresses in the flexures of similar magnitude.

The highest stress, 265 MPa, occurs in the jiggle axis flex-pivots. The 0.2% proof and ultimate tensile stresses and of 420S29 equivalent to the stainless steel used for these items are 555 MPa and 755 MPa respectively so the design appears relatively safe. It should be noted however that the model is a simplified representation for dynamic analysis and would need refinement for accurate stress calculation.

The load capacity of each of the pivots is 245 N (55 lb) and the weight of the jiggle and chop stages at 50g is 27 N.

L1n STRESS Lc=3

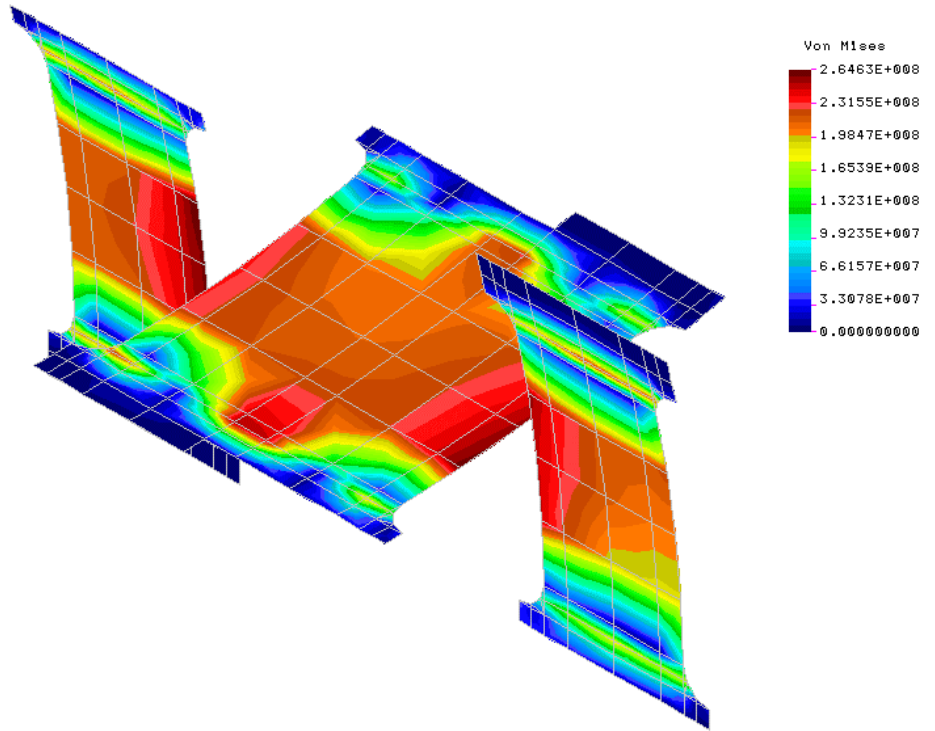


Figure 6-3: Flex pivot stresses from FEA

6.1.3 Flex Pivot Protection

Initial FEA work of the flex pivots has been performed to calculate stresses in flex pivots upon launch. Life issues, based on fatigue curves, are currently assumed to be as detailed in the manufacturer's technical data.

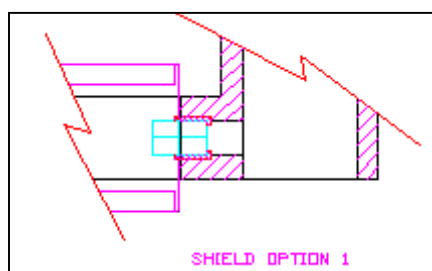


Figure 6-4 : Flex pivot protection sleeves, á la Goddard

To prevent damage by shear of the mechanism on launch a flex pivot capture sleeve, similar to this used by Goddard on COBE, will be utilised, as sketched above.

Based on holding the 0.036° requirement on the nominal (0,0) position, in the BSM specification a ~ 20 micron diametral clearance would be required on the approx. 80mm distance between pivots. This would prevent slop in the jiggle pivots producing an apparent chop motion, or vice versa. Without constraint, the standard flex-pivots would produce about +/-200um of slop (though we could get some manufactured with a tighter clearance). (Note this section needs updating in line with revision of the specification, SPIRE-ATC-PRJ-001 v2.0...relaxation to a +/-0.18° requirement will make this easier to achieve.)

Failure modes:


1. in the event of flex pivot failure, we could control position by motors alone and the random slop of the pivots would remain within spec.
2. In the event of motor failure (or launch damper failure to disengage), the flex pivots would provide self-centring (note that alignment of the centred position on integration will be critical, unless this is adjustable elsewhere in the optical path).
3. If both motors and pivots fail the position would be completely indeterminate, probably an end-stop out of the spectrometer FoV.

The argument against a latch is that the added protection against mission loss from this dual failure would be less than the risk of de-scoping to scan-mode only from a launch latch failure. Obviously, we need to get some numbers in to work this through properly. Another alternative (per GSW) would be to reduce the maximum chop axis throw, such that when its at its end stop half the FTS FoV is available ...This would be based on a trade off decision that there might not be too high a requirement to chop the full distance. GSW advises that mostly observers will do pixel-pixel chopping on small sources and scan map with (small) chop on the big ones, and there just aren't that many medium sources in the sky.

sleeves/bushes

One concern is that 20 um is too small a clearance (almost a light push fit) and would induce friction - especially if alignment(at 4k/ 0g) was not perfect to better than 5 um.

A second is that a working flex pivot produces some de-centring motion as it twists anyway : about +/-20um of linear motion in our case. We would arrange for this to be in the plane of the mirror (careful of course to install flex pivots in handed pairs, something which Goddard refer to as aligning the two pivots with the second pivot rotated 180°).

 <p>FIRST SPIRE</p>	<p>SPIRE Beam Steering Mirror Design Description v 3.4</p>	<p>Ref: SPIRE-ATC-PRJ-002 Page : Page 13 of 38 Date : 7.Feb.01 Author: Ian Pain</p>
--	--	---

That implies that our retaining 'bush' either needs to be slotted so that it has about 50um of lateral clearance - or that we use a top and bottom 'rail' rather than a bush.

One other failure mode could occur - the linear de-centre of the flex pivot is produced by a combination of opposing de-centre of each flex spring. If only one of them fails we assume that the de-centre will include an out-of plane component. e.g. if one chop pivot 'half failed' then a chop demand to the end-stop would also produce a 20um lift of that end of the chop axis (a small jiggle and a mirror translation of 10um upwards).

Given all the above : a capture sleeve with a 50-75um all round would still be desirable, (better than 400um!) but might may not fully meet the 0.036° spec. Note that it may be possible to have the flex pivots made with this clearance internally, as opposed to a bush or railing, but cost would be prohibitive.

6.1.4 Dynamics

The full report is found in document BSM Design Description v3_2.doc, see Appendix iii

6.2 The Support Structure (BSMs)

The design of the BSMs is less mature than that of the BSMm/BSMe as design responsibility was transferred to ATC from MSSL at a later stage. A simple aluminium alloy mount is envisaged with interface to the FPU optical bench will be via three shoulder bolts.

A 500g provision is made in the system mass budget (ref xxx), but a design goal of 250g will be adopted.

Although the BSMm provides for steering corrections and offsets, it remains desirable to provide precise location on the desired optical path such that a failure of the drive motors would leave the BSM in the failsafe position – ideally within 0.036 (NB may be 0.36 degrees only!) degrees of the nominal (0,0) position. [ref to the failsafe requirement which drives this xxx]. Classical high precision shoulder bolts would not provide sufficient accuracy to achieve this aim, and instead will be used to locate a mounting ‘shoe’ with three machined pads, as commonly used in ATC cryogenic mechanisms. The BSMs proper will mount to this shoe, with precise location (and the provision for one-off corrective machining) provided by mounting against the pads.

The additional benefit of this shoe is that the BSM may be removed during AIV troubleshooting as a complete unit. The drawback of an additional interface is poorer thermal conductivity and increased mass, and alternate schemes may be considered if this proves unwieldy.

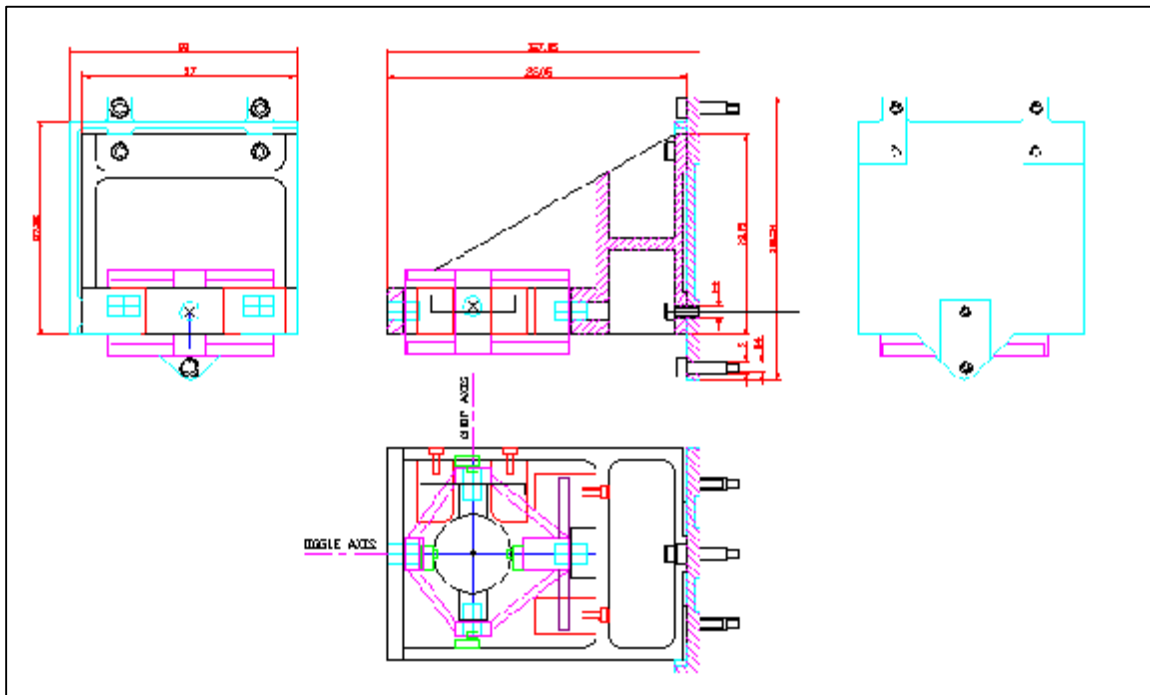


Figure 6-5 - Additional sketch of BSMs showing proposed mounting ‘shoe’ concept.

The BSMs provides for mounting of the:

- jiggle stage flex-pivots,
- jiggle stage sensors
- the jiggle and chop stage motors
- thermometry
- calibration source (ref to ICD with QMW) – for which a fairly large ‘optical bench’ area is provided to the rear of the mirror
- harness and connector mounts

The BSMs as drawn above assumes a doweled top clamp to retain the jiggle stage flex pivots, but a more elegant solution will shortly be implemented to split the mount in an analogous fashion to the jiggle framework.

The BSMs ICD to the structure will note:

- dimensional accuracy,
- CoG accuracy,
- mass accuracy,
- vibration (eigenfrequency)
- UNS fasteners to bench – sleeved dowels or fitted bolts (pref.)
- ALIGNMENT (0.036deg based on fail safe neutral position)

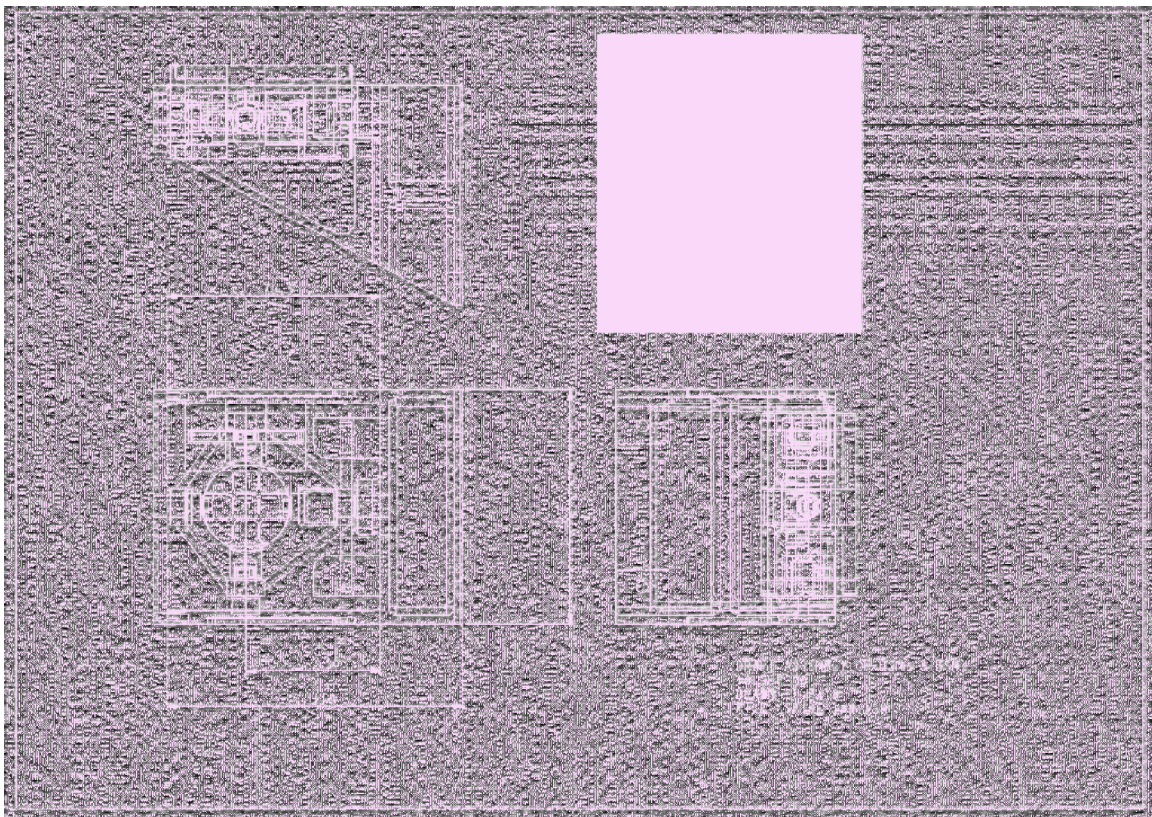


Figure 6-6 : BSMs and BSMm, assembly drawing from Pro/E model capture.

Figure 6-7: BSMs and BSMm, assembly drawing from Pro/E model capture.

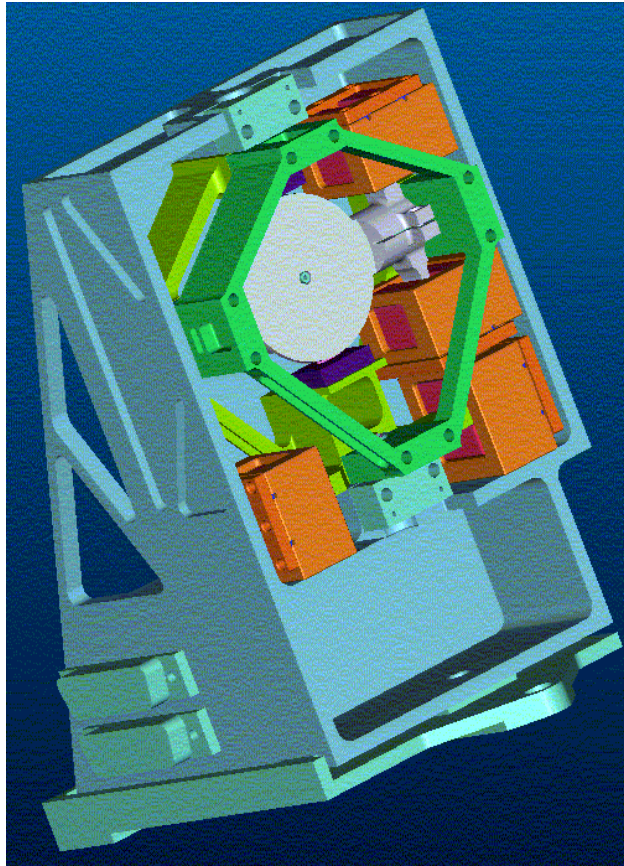


Figure 6-8 BSMm and BSMs. 3D view from Pro/E model looking onto the mirror surface. Jiggle frame in green, coils in orange, sensors dark blue.

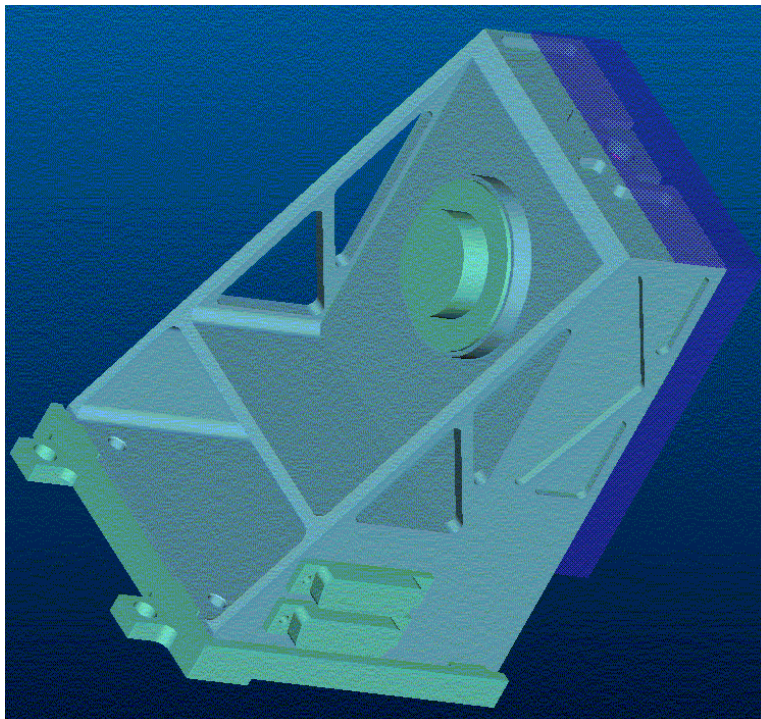


Figure 6-9: BSMm and BSMs. 3D view from Pro/E model looking from the rear. The PCAL unit is shown mounted at to the flat surface to the rear of the jiggle frame and motors.

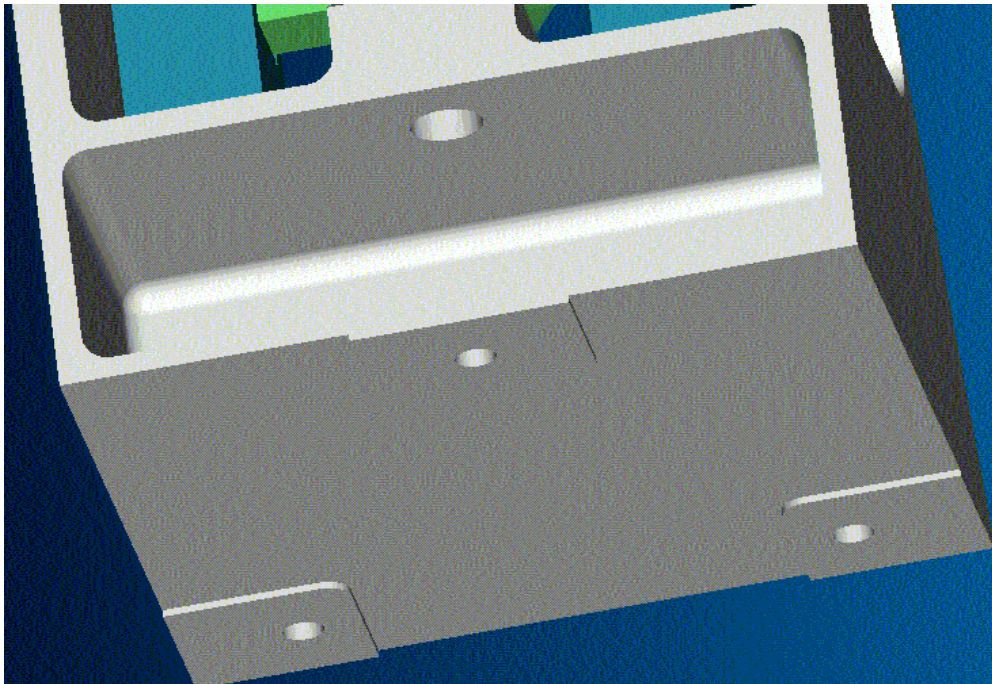


Figure 6-10: Additional 3D view of BSM, showing mounting surface on underside. This interfaces to the proposed mounting 'shoe'

6.2.1 Fasteners

Fasteners will all be of locking type. These may need to be UNS to find elliptical closure (preferred as they can't be assembled without locking) or lock-nut type (TBC). Thread lock will not be used, partly as it is not an ESA favourite, mainly as subsequent verification by inspection is difficult.

- All fasteners will be a cryogenic grade stainless steel.
- The mirror is machined integral to the chop stage, and a diamond turned or flycut finish is assumed.
- For science purposes a finish of ??? is required.
- For alignment purposes an optical finish of 10nm rms. is required (check rms. or Ra?)
- The Mirror is oversize (by 1 mm ... TBC)

6.2.2 Materials

The chop axis and integral mirror will be manufactured from Aluminium alloy grade 6061-T651, with intermediate heat treatments to stabilise the surface on cryogenic cycling per ATC specification (xxx)

The BSMs and any mounting shoe will be aluminium grade 6082 to match the MSSSL optical bench.

6.2.3 Thermal Strap Connection

One area of concern is thermal path through to the mirror. ISOPHOT saw a 120K differential on cool-down (through a single set of flex pivots). The jiggle stage sensor cables will provide some thermal path, and a thermal end-stop will be adopted as with the PACS chopper to provide an additional cooling path. During cooldown the chop and jiggle stages will be driven to the end of travel, where the end-of travel end stop will be designed to provide adequate thermal contact for cooling .

A flexible wick to the mirror may be required if this is insufficient.

A provision will be made on the BSMs bracket for a thermal strap tapping against the eventuality that thermal straps are required in addition to connection to the SPIRE optical bench.

6.2.4 Baffle and Light tight enclosure

A baffle is not formally part of the ATC work scope (TBC), but design integration of the baffle and structure must be considered at an early stage.

If adopted, a baffle will need to be displaced forwards of the BSM mirror due to the chop axis counterweight tabs (potentially a problem as the beam is strongly divergent)

A baffle needs to be substantial enough to maintain definition and alignment.

A light tight enclosure is a requirement on the BSM

The light tight enclosure will not require high structural definition - adequate only to survive installation & launch. Bent sheet metal probably best, not machined box (heavy/costly) nor foil (flimsy).

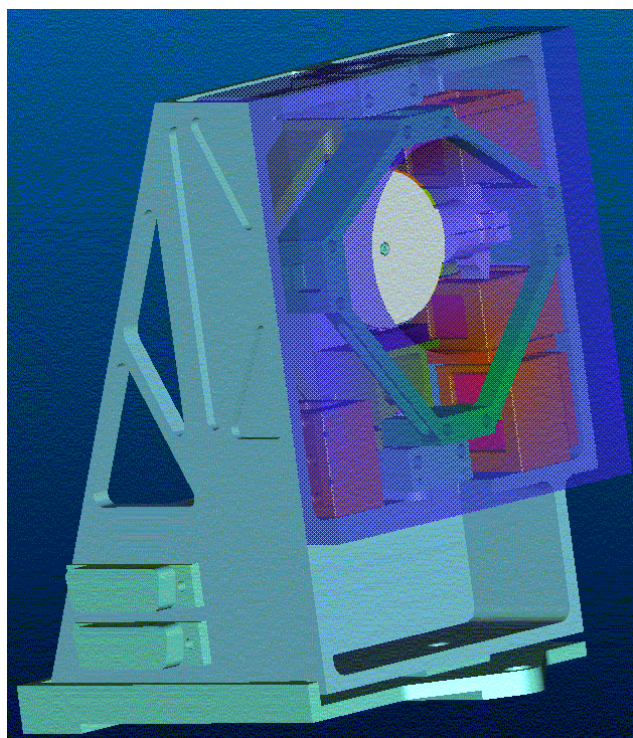


Figure 6-11: BSM shown with a conical baffle concept (shown semi transparent for clarity)

7. BSM Electronics & Controls

7.1 Control System Design

7.1.1 Parameters

Details to follow from B.Stobie

7.1.2 Dynamic Analysis

Figure 7-1BSM jiggle axis simplified dynamics with digital controller

7.1.3 Frequency analysis

The mechanical FE model was analysed to obtain the first 50 natural frequencies. The resonant frequencies of the chop and jiggle stages are 23 and 18 Hz respectively.

The first parasitic resonance occurs at 729 Hz.

FREQUENCY NUMBER	FREQUENCY (RAD/SEC)	FREQUENCY (CYCLES/SEC)	PERIOD (SECONDS)
1	.1142200E+03	.1817867E+02	.5500952E-01
2	.1454493E+03	.2314898E+02	.4319844E-01
3	.4577739E+04	.7285698E+03	.1372552E-02
4	.5822649E+04	.9267033E+03	.1079094E-02
5	.7800567E+04	.1241499E+04	.8054781E-03
6	.9250813E+04	.1472313E+04	.6792036E-03
7	.1019618E+05	.1622772E+04	.6162294E-03
8	.1030486E+05	.1640069E+04	.6097305E-03
9	.1129106E+05	.1797028E+04	.5564743E-03
10	.1459196E+05	.2322382E+04	.4305923E-03

7.1.4 Damping

The damping ratio for the near rigid-body modes (chop and jiggle) were set to 0.0004 based on data in the Lucas flex-pivot catalogue. For the higher frequency where the flexure of the jiggle-stage framework is significant the ratio was set to 0.02 which is typical of a well engineered bolted structure.

Set no.	First Mode	Last Mode	Damping Ratio
1	1	2	.4000E-03
2	3	50	.2000E-01

7.1.5 Chop axis excitation

Forces were applied equivalent to a couple of 1Newton forces acting at the chop magnet radius (15mm from the axis).

Below the resonance the response tends to the static case; a rotation of 0.086 radian.

+/- 1 NEWTON Z DIRECTION EXCITATION BY CHOP AXIS COILS

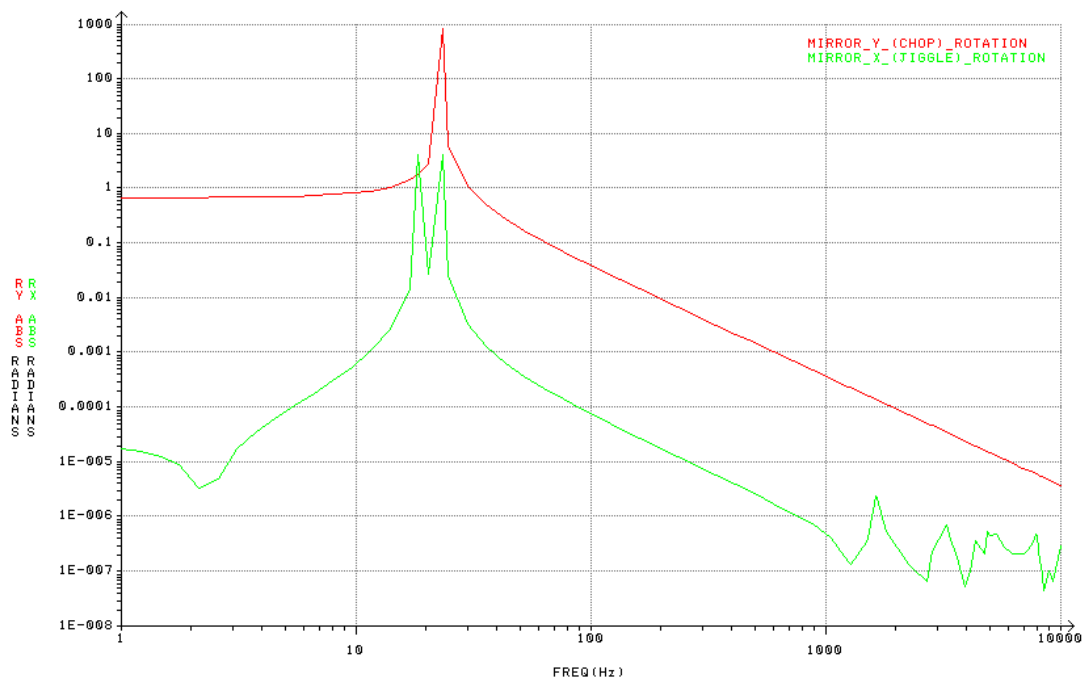


Figure 7-2: Chop axis excitation

+/- 1 NEWTON Z DIRECTION EXCITATION BY CHOP AXIS COILS

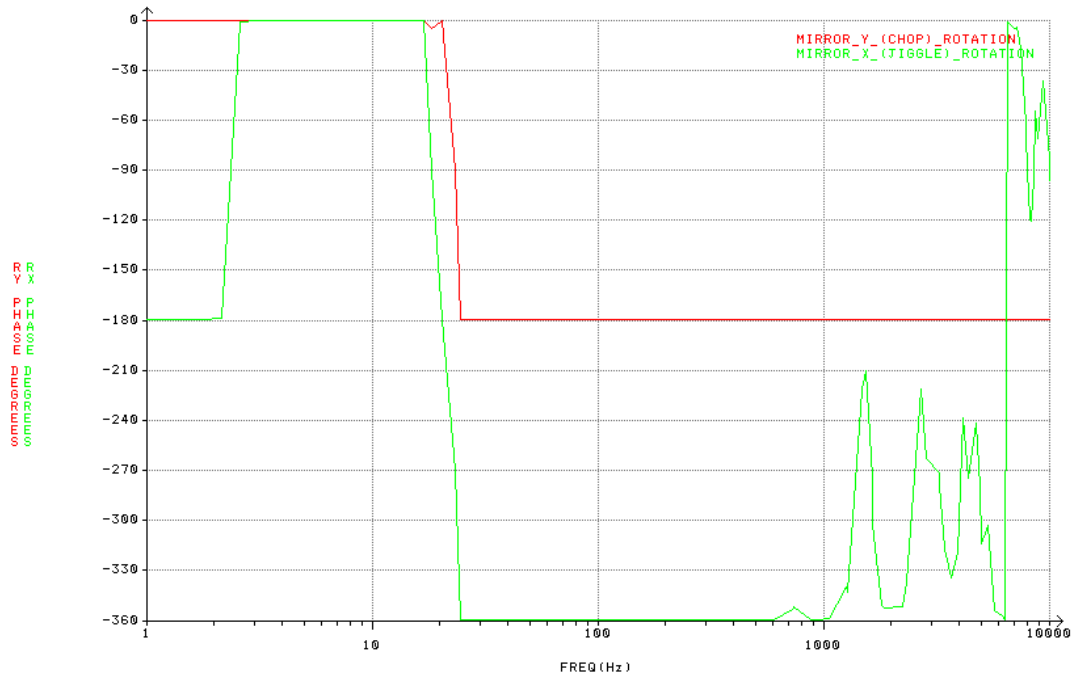


Figure 7-3: Chop axis excitation

7.1.6 Jiggle axis excitation

A couple of 1Newton forces acting at the centre of the jiggle magnets. Below the resonance the response tends to the static case; a rotation of 0.14 radian.

+/- 1 NEWTON Z DIRECTION EXCITATION BY JIGGLE AXIS COILS

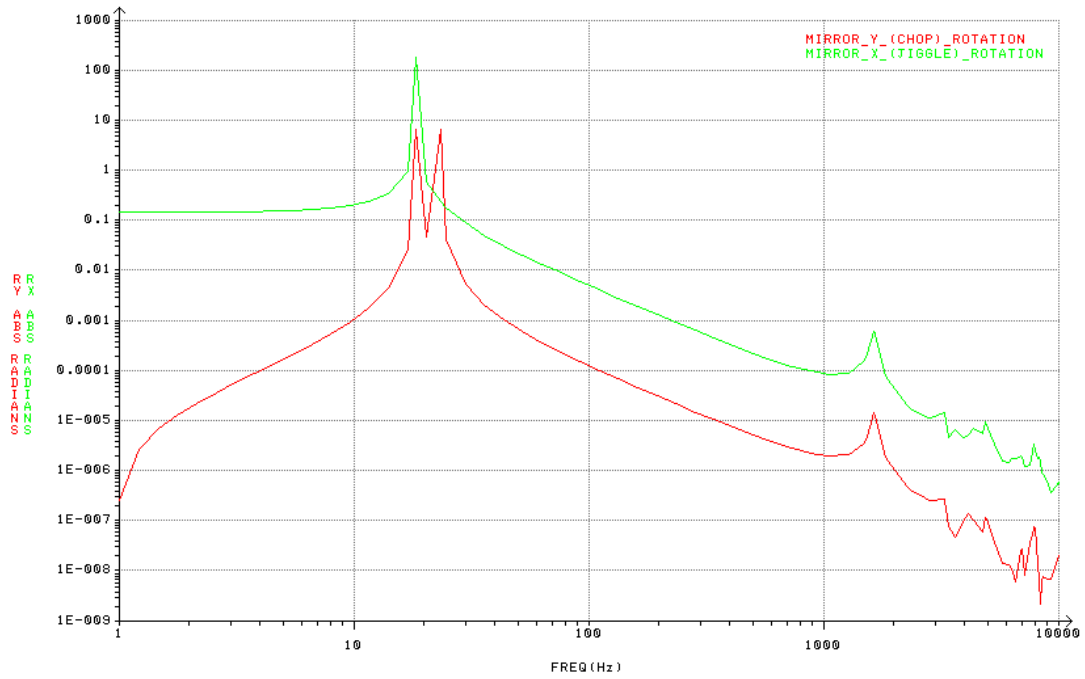


Figure 7-4: Jiggle axis excitation

+/- 1 NEWTON Z DIRECTION EXCITATION BY JIGGLE AXIS COILS

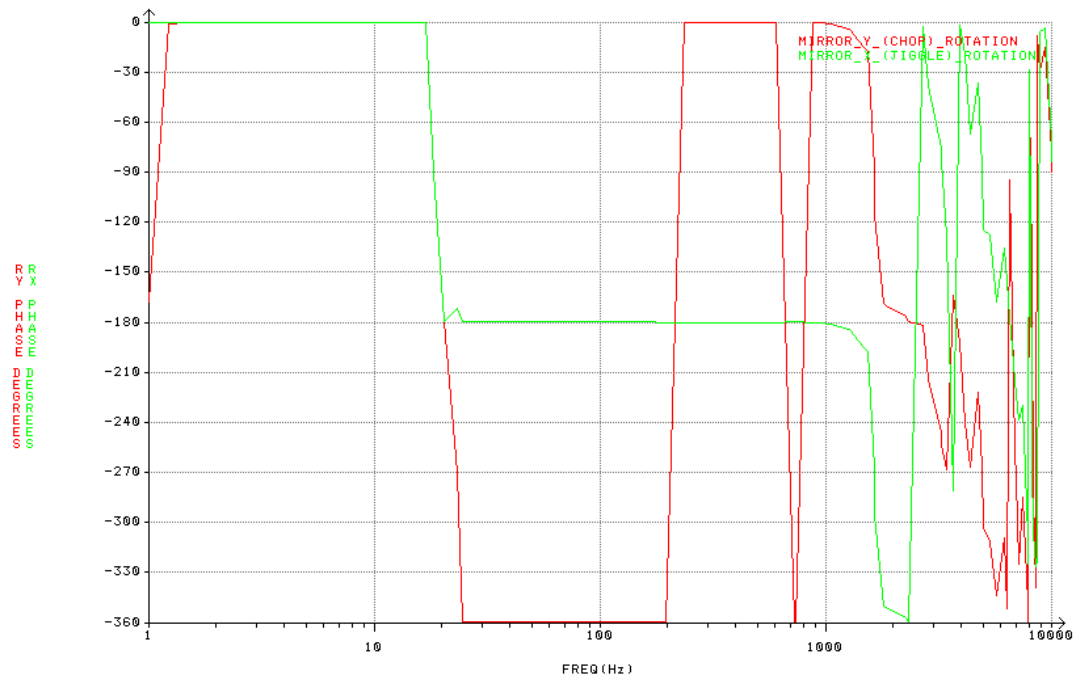
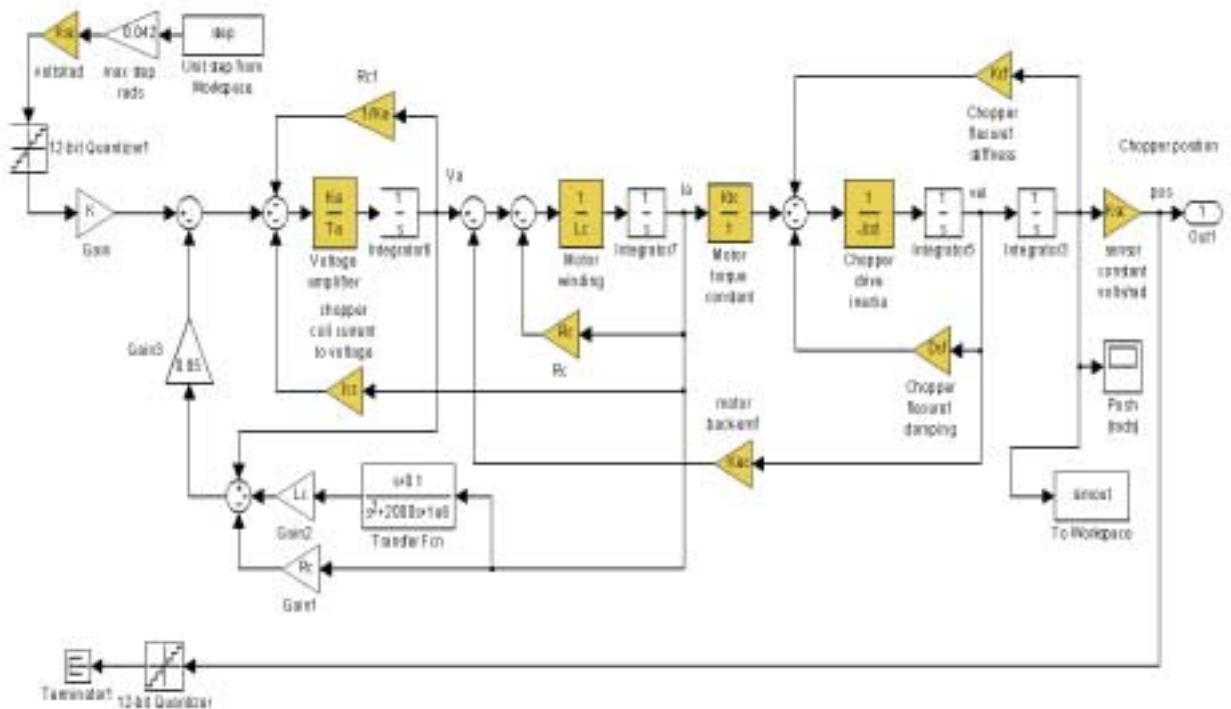


Figure 7-5: Jiggle axis excitation

7.1.7 Simulink Model

Full details of model & parameters need to be obtained from B.Stobie

7.1.8 Predicted Performance



SPIRE Beam Steering Mirror chopper axis simplified dynamics with no position feedback and estimated velocity damping:
spire_chop_mod6nofb.mdl

Figure 7-6: BSM chop axis simplified dynamics with no position feedback and estimated velocity damping.

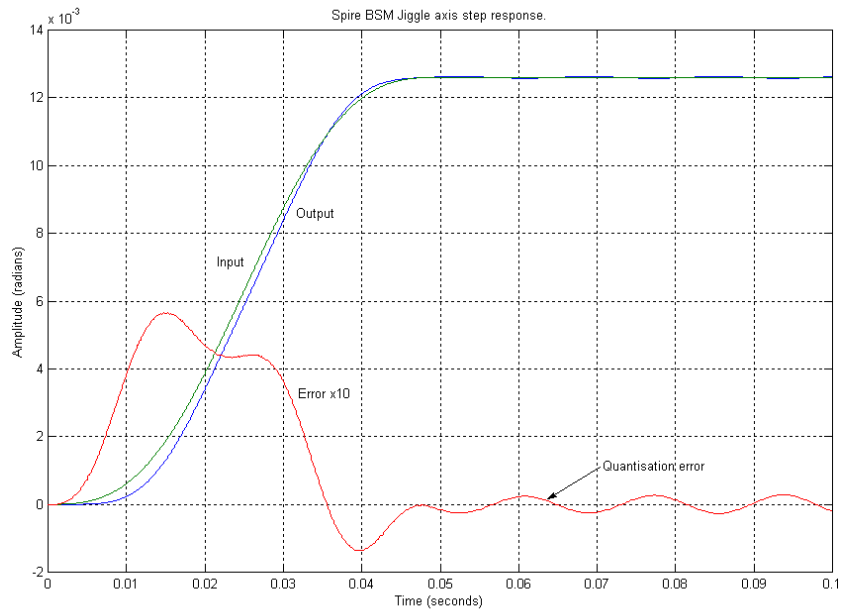


Figure 7-7: Jiggle axis step response.

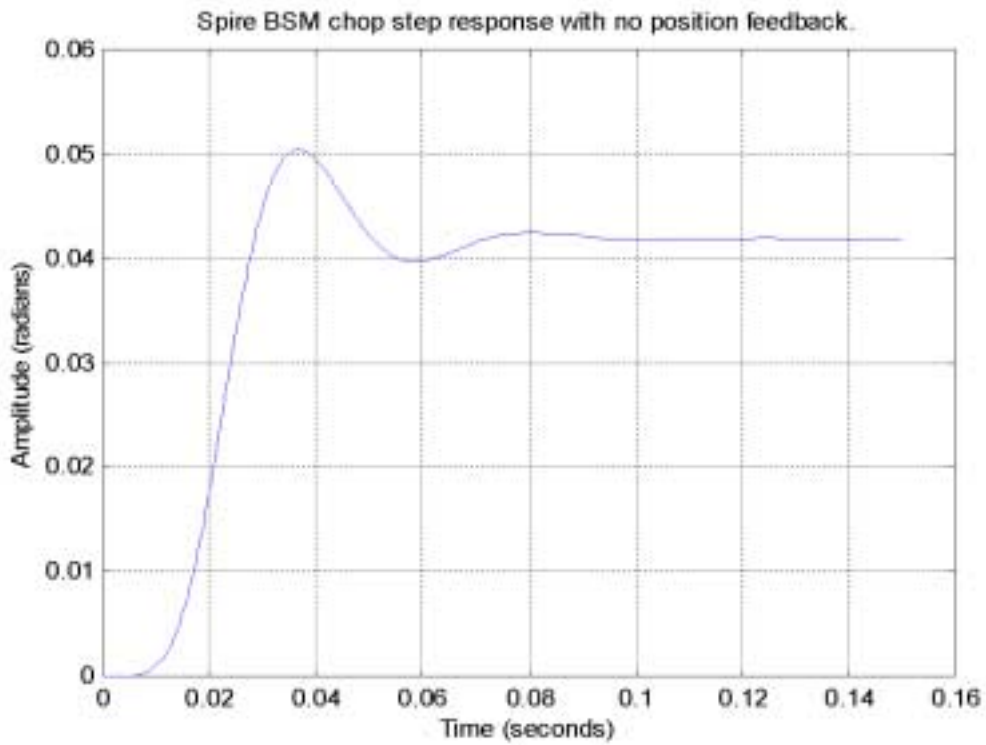


Figure 7-8: Jiggle axis step response.

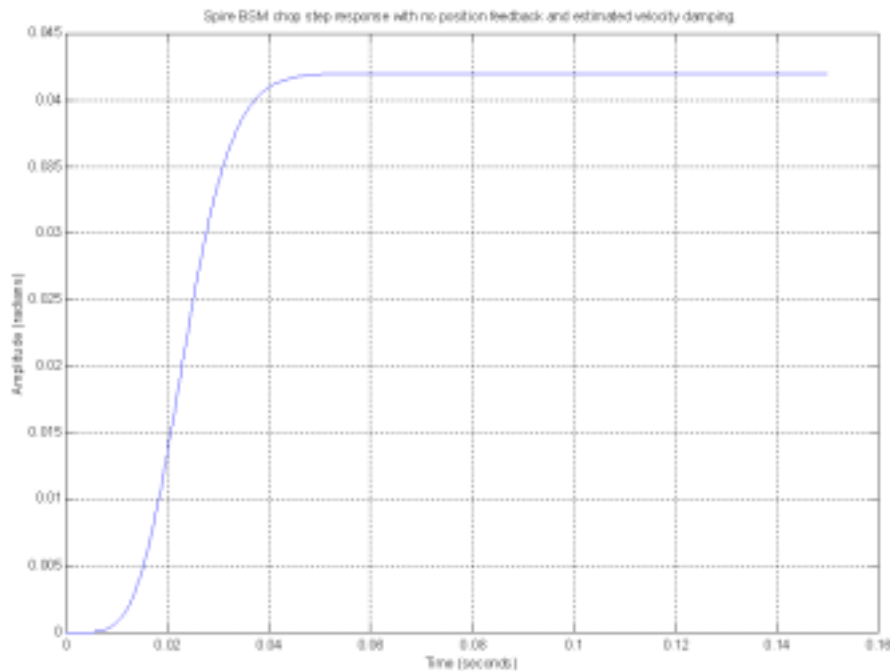


Figure 7-9: step response with no feedback

7.1.9 Power dissipation

The power dissipation of the BSMm and the BSMs shall be less than 4mW when operating in any mode at the nominal temperature. The average power dissipation of the BSMe shall be no greater than **TBD mW** when chopping at 2Hz in any operating mode.

7.1.10 Rise time

The chop axis, when driven with a smoothed trajectory demand has a predicted rise time of approximately 0.025 seconds, meeting the requirements.

7.1.11 Positional Stability

After settling, the mirror position shall remain within 0.004° rms. of the mean steady state position in the frequency range 0.03-25Hz.

7.1.12 Gain and Phase Margins

graphs to follow below. See appendix iii for more up to date data

Figure 7-10 Gain and Phase Margins for a) Chop axis and b) Jiggle axis

7.2 BSM Electronics

7.2.1 Block Diagram

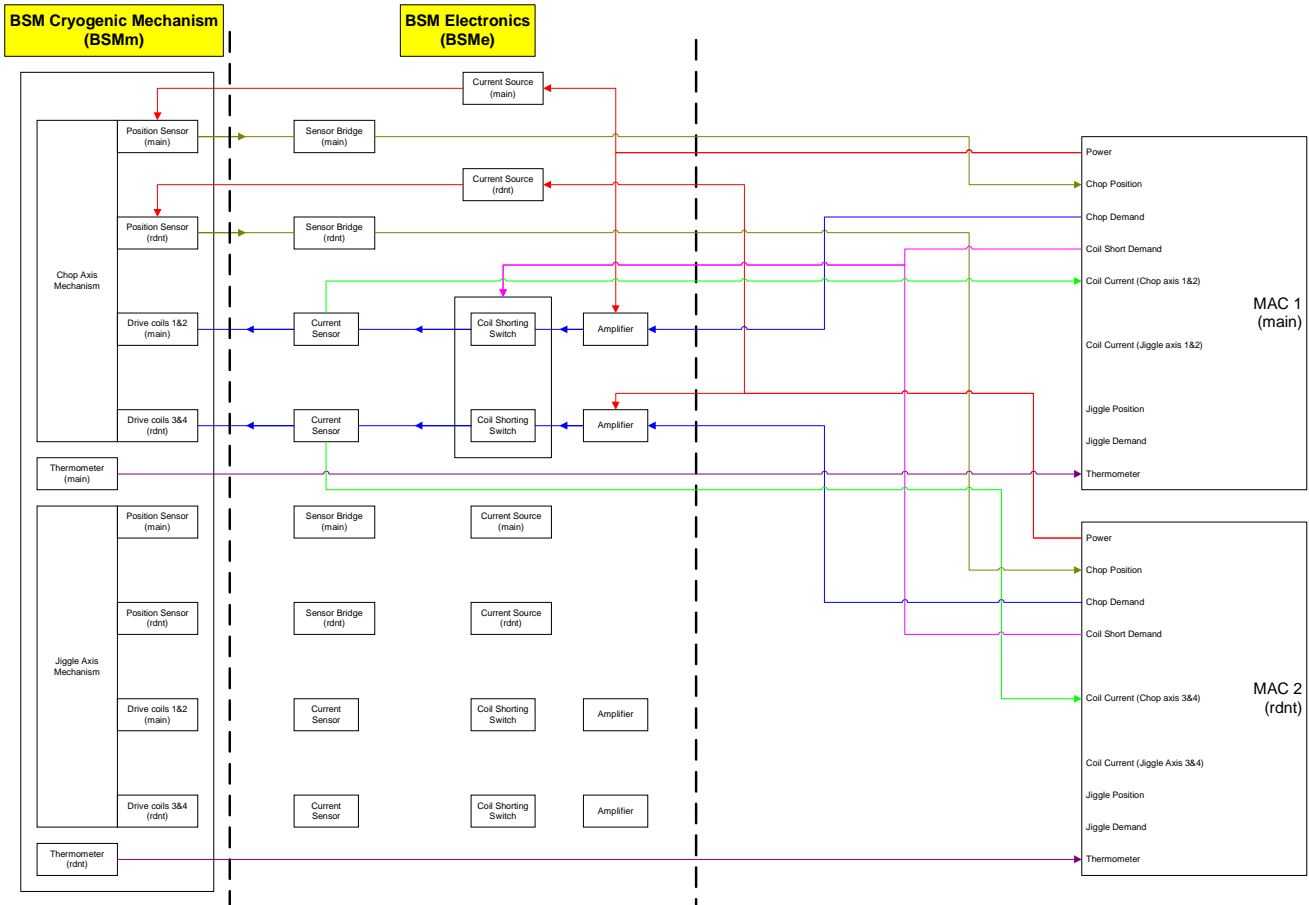


Figure 7-11: the basic architecture of the BSM Chop Axis, this is duplicated for the jiggle axis

Fig 8.1 demonstrates the core architecture of the BSM electronics. Both the main and redundant circuits for the chop axis mechanism are shown. The baseline scheme is to use a parallel redundancy method so that failure of any element, e.g. a coil, sensor or thermistor will result in the system being switched to the redundant MAC and power supply. (note though, that a switch may equally be required by a single failure of an element in the SMEC unit).

The launch latch/damper for both the main and redundant coils on each axis are released using a short coil demand line from either MAC. This diagram would imply a single point failure if there was a problem with the control wire, but a more detailed scheme is described below in Figure 8.2 overleaf.

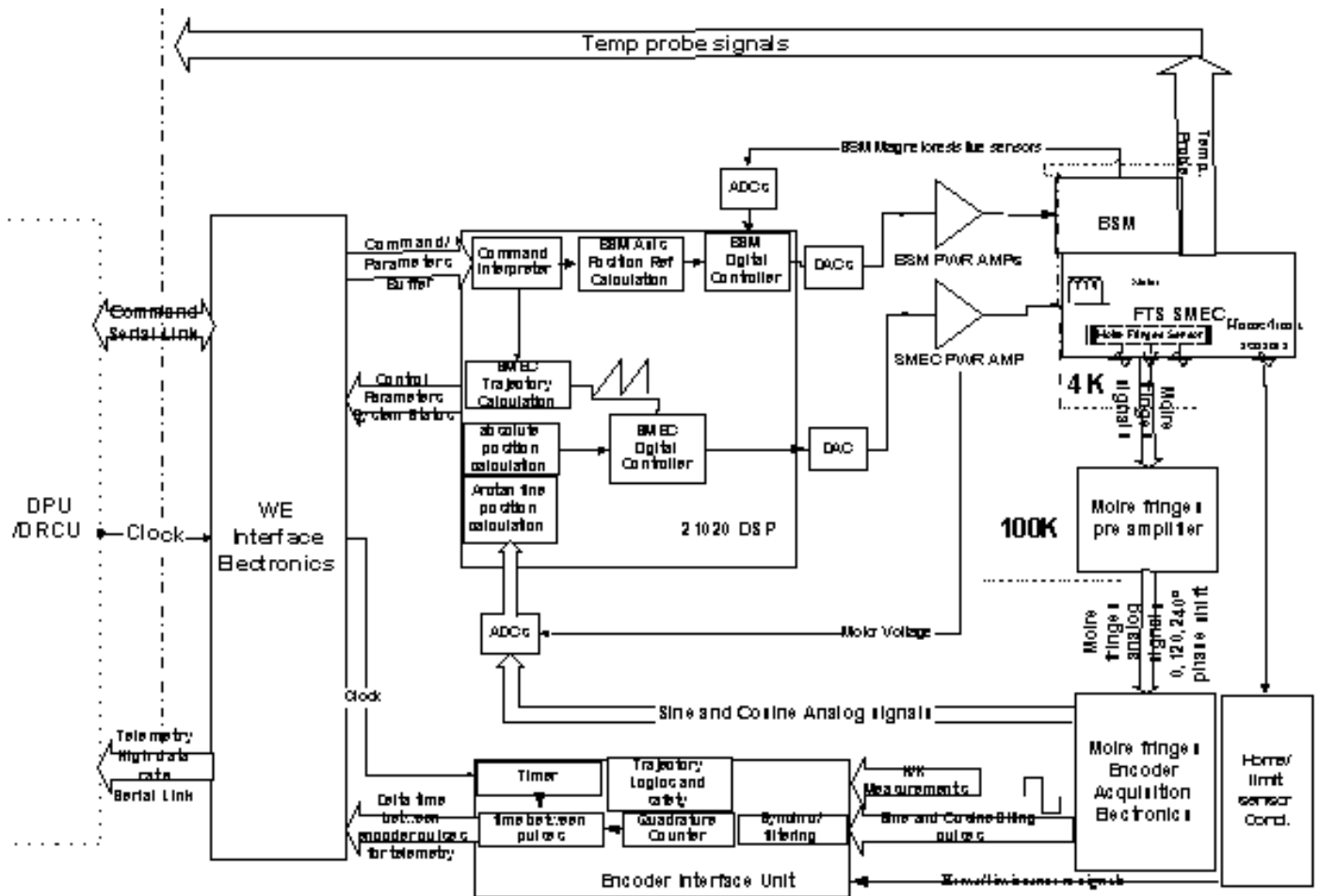


Figure 7-12 Incorporation of the BSM electronics within the

7.2.2 BSM Board

Similar to SMEC, the BSM Board is a double eurocard containing all the analogue electronics required for the BSM subsystem interface to the MAC. As an alternative – the BSMe requires little area and could be positioned on the SMEC card. This decision will be made after more detailed circuit design of both the BSMe and SMEC. The BSMe will include:

- ❖ Motor power amplifiers, providing the motor drive signals
- ❖ Coil current sensing
- ❖ Position sensor supply and bias

NB the SMEC document may imply that the main and redundant electronics may be included on the same board, but are to be supplied via different connectors to the primary and secondary MACs. This needs checking as it could be the cause of a single point failure if the connectors or board failed. Ideally, the primary SMEC and primary BSMe will be placed on a single board and the redundant BSMe and SMEC on another

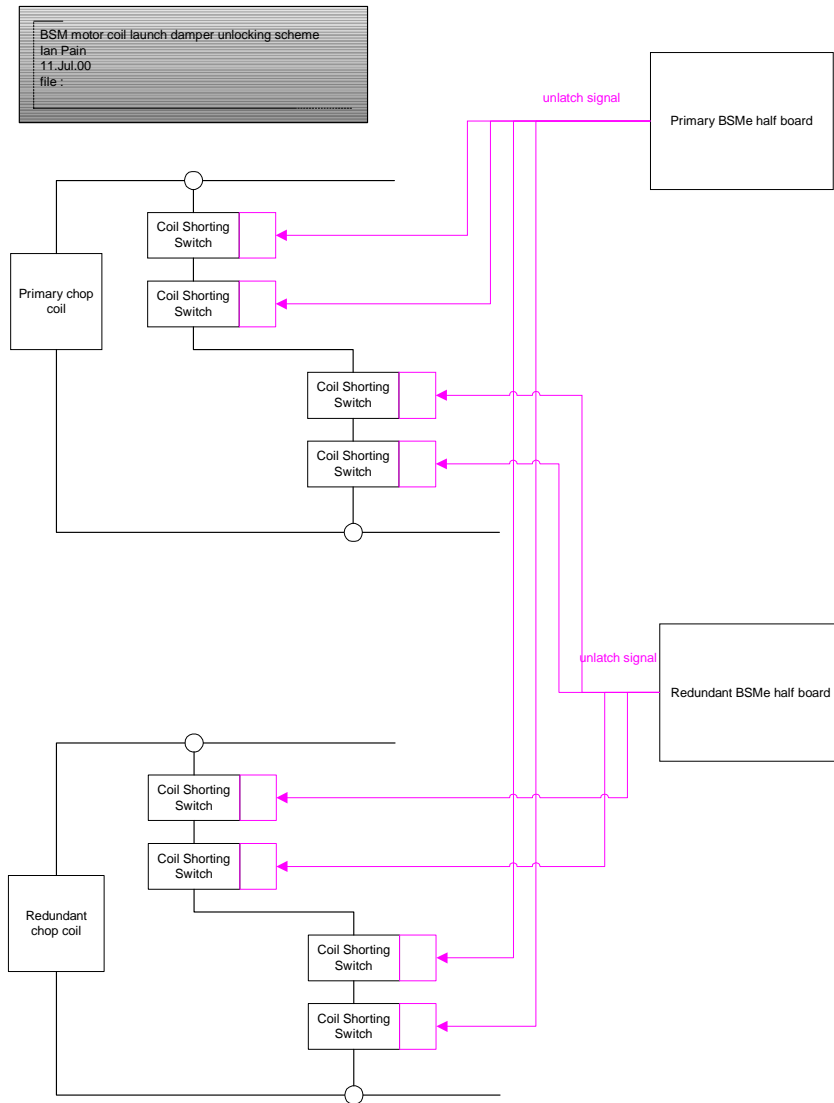


Figure 7-13: Launch Latch/Damper Scheme

7.2.3 Position sensors

For control of mirror movements, the drive system includes a position sensor for each axis to measure the inclination of the mirror in each axis. The signal is passed to the **MAC where an AFC system uses this to adjust the current in the motor coils**. The magneto-resistive position sensor chosen for this purpose will be similar to that used in the ISOPHOT mechanism, data sheet in Appendix ii. The sensors are dual InSb/NiSb magnetoresistive elements, biased with a permanent magnet and forming part of a bridge circuit. The voltage out against distance waveform is approximately sinusoidal.

7.2.4 Position sensor read-out circuits

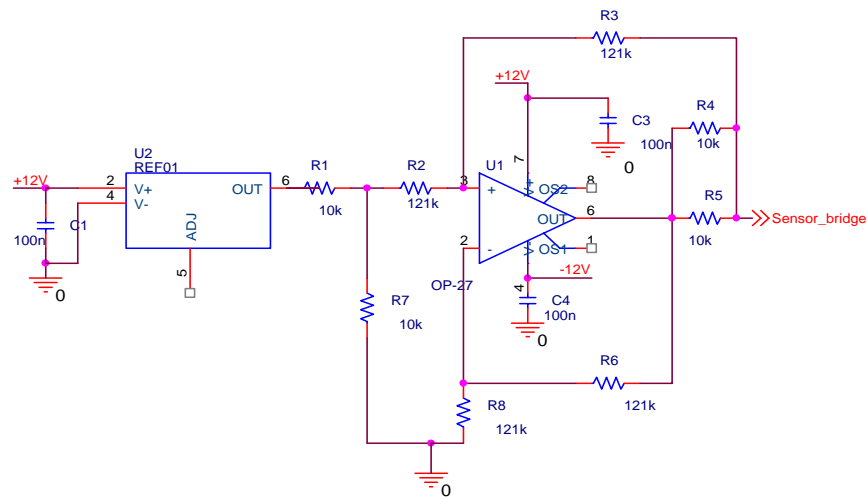


Figure 7-14 Current source (as used in ISOPHOT.)

The current source used in the ISO mechanism may have some issues with current drift as the circuit warms (or this may be problems with the ATC power source... work continues).

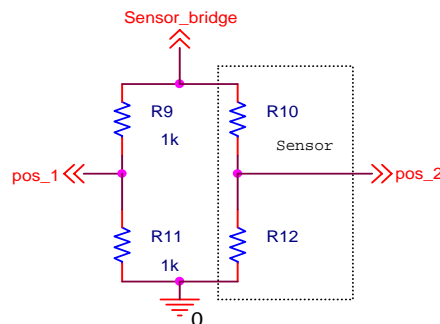


Figure 7-15 Position sensor bridge

The jiggle stage position sensor is located on the non moving housing of the BSMm The current source supplies current to the sensor bridge circuit with a **twisted screened pair** from the BSMe board to the BSMs. The other half of the bridge is situated with the BSMe (this may change if there is

room for them to be placed close to the sensor on the BSMm as this could reduce Johnson noise injected into the instrument amp).

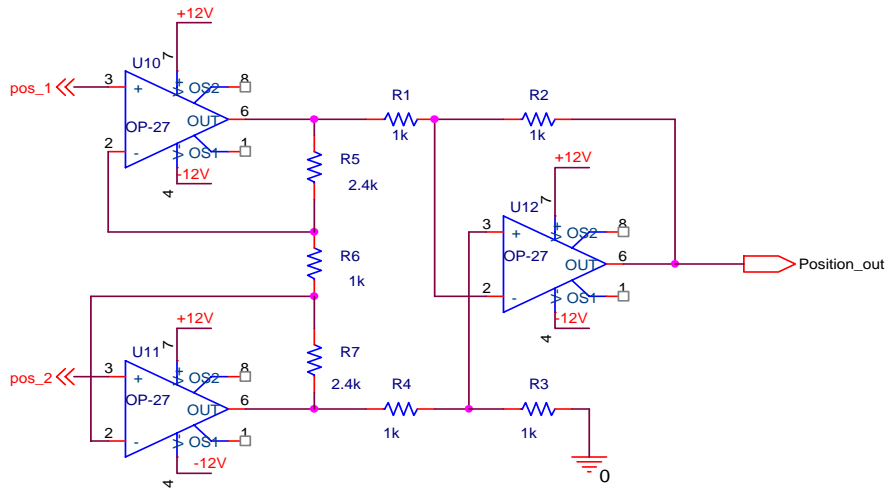


Figure 7-16 Instrumentation Amplifier.

The classic instrumentation amplifier shown in figure 8.4 takes in a differential signal from the centre points of the two arms of the sensor bridge. The circuit is designed with a high CMRR to reduce the noise common to both inputs injected into the circuit. This is a possible reason why the bridge circuit should be located in the same place so external noise affects both inputs. The position – voltage curve expected from the sensor will be supplied by F.Hannon.

7.2.5 Motors

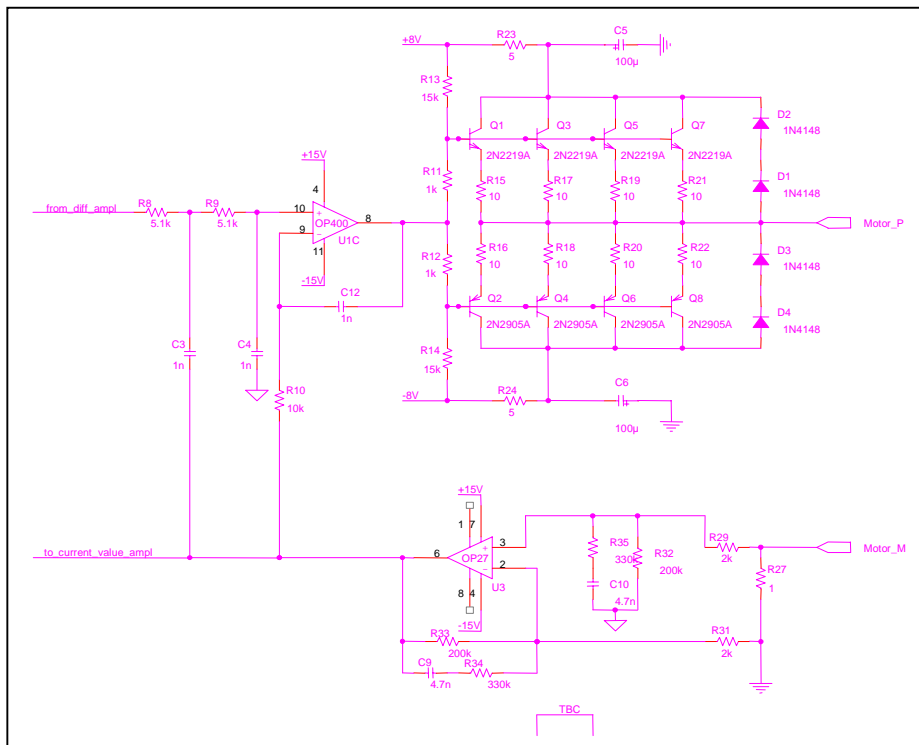


Figure 7-17 Motor Power Amplifier (as for SMEC)

The aseline design presented at PDR was that the coils used in the BSM would be the same as those used in ISO. However, lack of configuration documentation for these items makes it impractical to duplicate them. The newly proposed baseline is that the BSM will use the motor coils being developed for PACS.

Each axis will have 4 coils (2 main, and 2 redundant). Th eredundancy will be ideally aranged so that pure torque is generated . .

It is a concern however that there may be a certain amount of cross talk between the coils induced magnetic flux and the magneto resistive position sensors. It could be arranged that the main position sensor for each axis is closer to the redundant coil and vice versa so as to try and keep the effects to a minimum. Motor power amplifiers

The motor amplifier as provided by SMEC, Figure 7-17 may have some associated reliability issues.

7.2.6 Thermometry

The operating temperature of the BSMm will be 4K and the mirror or structure is to rise by no more than 1K from the nominal operating temperature.

The temperature of the cold electronics will be monitored using a CX-1050 copper canister resistance temperature sensor, calibrated to be sensitive over the 1.4K to 325K region. The maximum temperature rating is 325K, as shown in the data sheet Appendix ii, but as the specified soldering temperature exceeds this, no particular concerns are identified for bake-out at 353K.

7.2.7 Power Supply

Subsystem	Nominal Voltage	Average Current	Peak Current/ time	Voltage Stability	Voltage Noise	Remarks
MAC board DSP and Logic	+ 5 V	1.6A	2.7 A / 100 ms	± 2.5%	TBD	
MAC board Analogue and data converters	± 15 V	90mA (on +15V) 77mA (on -15V)		± 2.5%	TBD	
BSM board Motor Amps	+ 8V	10 mA	100 mA/ 50 ms	± 5%	TBD	Voltage depends on motor harness resistance at 300K
BSM board Analogue Electronics	+ 15 V	50mA (on +15V) 50mA (on -15V)		+ 2.5%	TBD	

Two complete sets of these power lines are required to satisfy the main and redundant power lines. All electronic components in the BSM mechanism are powered from the BSM board. REF – First/Spire/SMEC Electronics Design Description

7.2.8 Grounding Scheme

TBD

EMI/EMC effects are reduced by implementing when applicable dual balanced electrical interfaces.

7.2.9 Harness/ Cables

The wire count for the BSM harness is shown below in the table. The number of wires takes into account those used for both the main and redundant systems.

DIAGRAM TO GO HERE (F.HANNON/B.STOBIE)

Location	Item	Number of Wires
BSMe and BSMm	Position Sensors	16
	Thermometers	4
BSMe and MAC	Control and sense lines	16
	Power (incl. motors)	32

7.2.10 Interface to Digital Controller

Something to go here ? check with F.Hannon/ B.Stobie

8. Reliability & Redundancy

In the BSM design redundancy principles have been implemented so as to avoid single point failures, and the propagation of failures to other subsystems by means of dedicated redundancy and specific protection devices. Where redundancy can not be realised the architecture is designed to limit the effects of a failure.

The prime BSM redundancy option consists of two separate circuits (possibly situated on the same double eurocard). This provides complete parallel redundancy, with main and redundant position sensors and motors, driven by separate main and redundant analogue boards, which are in turn supported by main and redundant MACs and DPUs as shown in Figures 8.1 and 8.7.

The BSM redundancy scheme will not be able to operate independently of the SMEC mechanism, A failure in the primary system of either mechanism results in both switching to the redundant schemes (TBC). An alternative redundant method is described in Appendix i.

8.1 Reliability Block Diagram

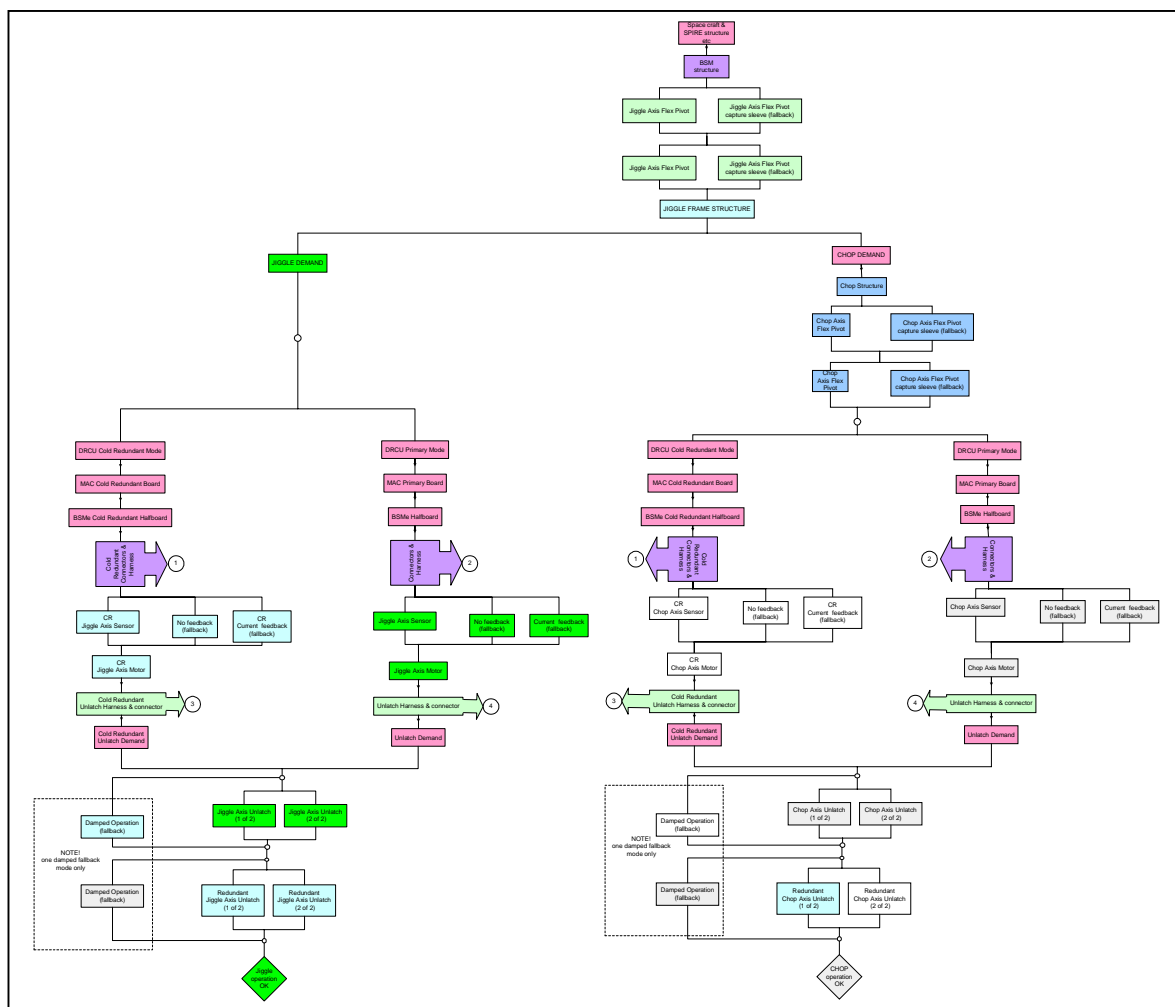



Figure 8-1 Reliability Block Diagram

 <p>FIRST SPIRE</p>	<p>SPIRE Beam Steering Mirror Design Description v 3.4</p>	<p>Ref: SPIRE-ATC-PRJ-002 Page : Page 34 of 38 Date : 7.Feb.01 Author: Ian Pain</p>
--	--	---

A Reliability Block Diagram is considered above. At this level it is apparent that

1. Wiring harness is a potential Single point failure, unless both the BSMe 'half' boards have an individual cable harness with it's own connectors. This was probably how we would have implemented it anyway but we should remain wary of combining the harness into a single connector at any point.
2. The BSM structure and jiggle frame are SPF's. No surprise, but it reinforces the requirement for analysis of these structures for survival, and possible additional tests (e.g. to verify the FEA).
3. Assuming we have a launch damper (shorted motor coils), In the primary operations mode the launch damper 'unlatch' command must unlatch the primary mode motor coil, BUT MUST ALSO unlatch the cold redundant motor coils latching circuit. Vice versa for the redundant mode. This was already in the BSME schematic Subsystem Specification Document (Beam Steering Mechanism, Figure 4)
4. The same comment as (1) applies for the cables which send the unlatch command - they should remain separate and parallel. There was a hint in an early the schematic that the primary and redundant connectors would join before the unlatch switch, or share an unlatch switch ... which would be bad.

9. Command modes

9.1 *Command List*

Commands and Related Parameters	Action	Comment
To be completed see GSW		

Appendix i.

An alternative redundancy method being considered is a non parallel architecture that enables the BSM to still operate on its main system whilst the rest of the mechanism has switched to the redundant scheme. This could however be the cause of a single point failure as the complexity increases with the need for additional circuitry as demonstrated by Fig 11.1.

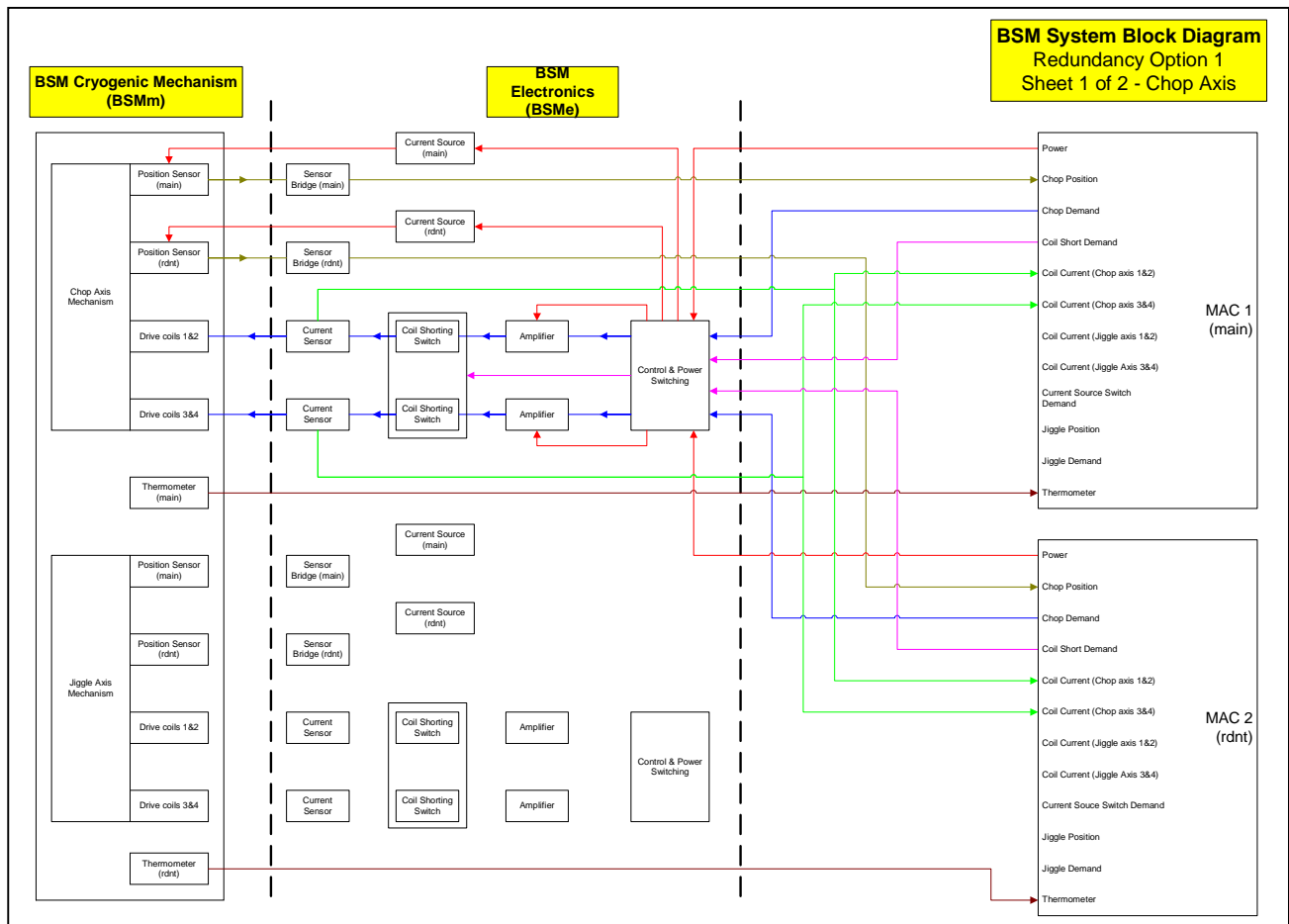



Figure 0-1 Alternative Redundancy Scheme

 <p>FIRST SPIRE</p>	<p>SPIRE Beam Steering Mirror Design Description v 3.4</p>	<p>Ref: SPIRE-ATC-PRJ-002 Page : Page 37 of 38 Date : 7.Feb.01 Author: Ian Pain</p>
---	--	---

Appendix ii

[CERNOX™ Resistance Temperature Sensor Data Sheet – technical spec – pdf document](#)

[Infineon Magneto-Resistive Sensor Data Sheet- FP 210 L 100-22 \(near the bottom of the page – pdf document\)](#)



FIRST

SPIRE

SPIRE Beam Steering Mirror Design Description
v 3.4

Ref: SPIRE-ATC-PRJ-002

Page : Page 38 of 38

Date : 7.Feb.01

Author: Ian Pain

Appendix iii Dynamic Analysis Of The BSM

(not attached electronically)

Document No: ATC internal: spire-bsm-001-tdn-001.doc.133

SPIRE: **to follow.**

Status: Draft

Version: 10

Modified by: Richard Bennett

Modified date: 4 May 2000 7:30 PM

Author: Richard Bennett

Created date: 4 May 2000 5:04 PM

Category: Technical Design Note

Type:

Generated with: Microsoft Word 8.0

File: spire-bsm-001-tdn-001.doc